

# An SAV Method for Imaginary Time Gradient Flow Model in Density Functional Theory

Ting Wang<sup>1</sup>, Jie Zhou<sup>2</sup> and Guanghui Hu<sup>1,3,4,\*</sup>

<sup>1</sup> *Department of Mathematics, Faculty of Science and Technology, University of Macau, Macao SAR, China*

<sup>2</sup> *School of Mathematics and Computational Science, Xiangtan University, Xiangtan, Hunan 411105, China*

<sup>3</sup> *Zhuhai UM Science & Technology Research Institute, Zhuhai, Guangdong 519030, China*

<sup>4</sup> *Guangdong-Hong Kong-Macao Joint Laboratory for Data-Driven Fluid Mechanics and Engineering Applications, University of Macau, Macao SAR, China*

Received 5 December 2021; Accepted (in revised version) 11 September 2022

---

**Abstract.** In this paper, based on the imaginary time gradient flow model in the density functional theory, a scalar auxiliary variable (SAV) method is developed for the ground state calculation of a given electronic structure system. To handle the orthonormality constraint on those wave functions, two kinds of penalty terms are introduced in designing the modified energy functional in SAV, i.e., one for the norm preserving of each wave function, another for the orthogonality between each pair of different wave functions. A numerical method consisting of a designed scheme and a linear finite element method is used for the discretization. Theoretically, the desired unconditional decay of modified energy can be obtained from our method, while computationally, both the original energy and modified energy decay behaviors can be observed successfully from a number of numerical experiments. More importantly, numerical results show that the orthonormality among those wave functions can be automatically preserved, without explicitly preserving orthogonalization operations. This implies the potential of our method in large-scale simulations in density functional theory.

**AMS subject classifications:** 65N30, 37M05

**Key words:** Density functional theory, gradient flow, scalar auxiliary variable, unconditional energy stability, orthonormalization free.

---

## 1 Introduction

The Kohn-Sham density functional theory (KSDFT) [13] is one of the most successful approximation models of the many-body Schrödinger equation. Thanks to the Hohenberg-

---

\*Corresponding author.

Emails: YB97467@um.edu.mo (T. Wang), zhouj@xtu.edu.cn (J. Zhou), garyhu@um.edu.mo (G. Hu)

Kohn theorem, the ground state electron density is used as a fundamental variable to describe the many-body problem. This is a huge reduction on the dimensionality since the ground state electron density is a three dimensional variable while the wave function in the original many-body system is a  $3N$  dimensional one. However, it is still very challenging to develop efficient numerical methods for the KSDFT, due to the singularity from the external potential, the orthonormality constraint for those wave functions, etc. Besides the popular self-consistent field iteration [22,23], minimizing total energy [10,26] is an alternative approach for the ground state calculation. In this direction, the gradient flow method is a competitive method due to its feature on energy dissipation, in which there have been many pioneer works on developing numerical methods [19,27,30]. Among all these methods, the emerging scalar auxiliary variable (SAV) method has been attracting more and more attention since its excellent performance in the simulation.

The SAV method has been proposed in [32,33] for solving the Allen-Cahn and Cahn-Hilliard equations. The main idea of SAV [25] is to introduce a scalar auxiliary variable which is a square root function to reformulate a gradient flow model into an equivalent form. For the reformulated system, it is easy to construct a linear scheme with unconditional energy stability, which in turn solves the original model. The original SAV method has the following remarkable features [17]: i) At each time step, only decoupled, linear systems with constant coefficients need to be solved (efficiency); ii) The first- and second-order SAV schemes are unconditionally energy stable (stability); iii) The form of nonlinear part of total energy is not restricted, so it applies to a large class of gradient flows (flexibility). Due to the above advantages, several works have been completed based on this method. The convergence and error analysis of the SAV method for gradient flow have been developed in [31]. The high-order scalar auxiliary variable (HSAV) method was presented in [16], and it has been shown that the newly proposed schemes could be reached in arbitrarily high order in time. In [7], the generalized scalar auxiliary variable method (G-SAV) was proposed where the definition form of the auxiliary variable was extended. More variants of the SAV method for solving Allen-Cahn type equations can be found in [20,21].

By using the method mentioned above, the SAV method has already been widely used in variable problems. In [29], a second order SAV Crank-Nicolson (SAV-CN) scheme was adopted to solve the Peng-Robinson EOS problem. In [1], a second order SAV pseudo-spectral scheme was proposed to handle the dynamics of general nonlinear Schrödinger/Gross-Pitaevskii equations. In [12], an SAV-Gauss collocation finite element method was used to study nonlinear Schrödinger equation. In [8], a second order SAV modified Crank-Nicolson scheme was proposed and analyzed for the epitaxial thin film growth model. Recently, in [35], a modified SAV scheme was constructed to solve the ground state solutions of one- and multi-component Bose-Einstein Condensates (BECs). It is mentioned that there is a norm preserving constraint in the problem, which is removed by the authors by introducing a penalty term in the expression of total energy. With this strategy, the unconditional decay of the modified total energy can be obtained both theoretically and numerically, while the norm constraint can be satisfied automatically.

It is known that in solving the original imaginary time gradient flow model in DFT, there is an orthogonality constraint for wave functions. It is this constraint which brings a nontrivial challenge for developing efficient numerical methods. There have been many pioneer works towards removing the orthogonalization from the algorithm, please refer to [9, 10, 14, 15]. Following the idea in [35], it could be feasible to handle the orthonormality constraint in the Kohn-Sham equation by introducing penalty terms, which motivates our work in this paper. However, to our best knowledge, there is few related work towards this direction.

In this paper, an SAV method for the ground state calculation of a given electronic structure system will be proposed and analyzed. Following the idea in [35], we write a modified Kohn-Sham energy functional in which two kinds of penalty terms are adopted to handle the orthonormality constraint of wave functions. And the corresponding imaginary time gradient flow model is reformulated by introducing three kinds of scalar auxiliary variables, i.e., one for the nonlinear energy functional, one for the norm constraint of each wave function and the last one for the orthogonality between each pair of different wave functions. We design a scheme for the temporal discretization and prove the scheme enjoys the unconditional energy stability property. It is worth pointing out that, different from the previous works, we find some relaxation on the conditions to guarantee the energy decay property. Together with a spatial discretization method, a full discretization scheme is established. To describe the external potential in total energy, we adopt the  $h$ -adaptive method, which is a successful method to describe the singularity with fewer mesh grids and widely used in variable problems [2, 4, 5, 24, 34]. Local density approximation (LDA) is used to handle exchange-correlation potential. To give the boundary values of Hartree potential, multipole expansion approximation is employed. The convergence and effectiveness of our method are demonstrated by several numerical experiments. It is worth mentioning that the orthonormality relationships among wave functions can be automatically preserved by our method, without explicitly preserving orthogonalization operations.

The rest of this paper is organized as follows. In the next section, firstly we introduce the Kohn-Sham energy functional, then an imaginary time gradient flow model is presented. In Section 3, a modified Kohn-Sham energy functional with some penalty terms is presented, as well as the SAV reformulation of the corresponding imaginary time gradient flow. Then the full discretization scheme is established. In Section 4, some numerical experiments are presented to validate the effectiveness of the proposed scheme. The conclusion is given in the last section, as well as future work.

## 2 The imaginary time gradient flow model

In this section, we introduce the original Kohn-Sham energy functional, then the corresponding imaginary time gradient flow model is presented. Below we start from the original Kohn-Sham energy functional.

Let  $\Omega \subset \mathcal{R}^3$ . We consider a molecular system consisting of  $M$  nuclei with charges  $\{Z_1, Z_2, \dots, Z_M\}$  and locations  $\{R_1, R_2, \dots, R_M\}$ , respectively, and  $N_{ele}$  electrons. The general Kohn-Sham energy functional takes the form,

$$E(\Phi) = \int_{\Omega} \left( \frac{1}{2} \sum_{i=1}^N f_i |\nabla \phi_i(r)|^2 + V_{ext}(r) \rho(r) \right) dr + E_{Har}(\rho) + E_{xc}(\rho) \quad (2.1)$$

for  $\Phi = (\phi_1, \phi_2, \dots, \phi_N)$ . Here  $N$  is the number of Kohn-Sham orbits,  $N = N_{ele}/2$  if  $N_{ele}$  is even;  $N = (N_{ele} + 1)/2$ , if  $N_{ele}$  is odd.  $f_i$  is the occupation of orbital  $i$ .  $\rho(r)$  is the electronic density defined by

$$\rho(r) = \sum_{i=1}^N f_i |\phi_i(r)|^2.$$

$V_{ext}(r)$  is the Coulomb potential defined by

$$V_{ext}(r) = - \sum_{k=1}^M Z_k / |r - R_k|.$$

The third term of (2.1) is Hartree energy

$$E_{Har}(\rho) = \frac{1}{2} \left( \int_{\Omega} \int_{\Omega} \rho(r) \rho(r') / |r - r'| dr' dr \right).$$

Its functional derivative with respect to  $\rho$  is Hartree potential defined by

$$V_{Har}(r) = \delta E_{Har} / \delta \rho(r) = \int_{\Omega} \rho(r') / |r - r'| dr'.$$

$E_{xc}(\rho)$  is exchange-correlation energy and its functional derivate with respect to  $\rho$  is exchange-correlation potential defined by

$$V_{xc}(r) = \delta E_{xc} / \delta \rho(r),$$

to which some approximations should be applied, such as LDA, GGA [13], etc. Actually, the total energy also has a nucleus-nucleus interaction  $E_{nn}$  defined by

$$E_{nn} = \sum_{I=1}^M \sum_{J>I}^M Z_I Z_J / |R_I - R_J|.$$

It can be observed that with fixed configuration of the position, the one is a constant, which will not affect our analysis. The ground state can be reached by minimizing the above energy. The minimization problem can be written as

$$\begin{cases} \text{Min } E(\Phi) = \text{Min} \left( \int_{\Omega} \left( \frac{1}{2} \sum_{i=1}^N f_i |\nabla \phi_i(r)|^2 + V_{ext}(r) \rho(r) \right) dr + E_{Har}(\rho) + E_{xc}(\rho) \right), \\ \text{s.t. } \int_{\Omega} \phi_i(r) \phi_j(r) = \delta_{ij}, \end{cases} \quad (2.2)$$

where  $1 \leq i, j \leq N$  and  $\delta_{ij}$  is the Kronecker Delta symbol. Assume the total energy functional (2.1) is bounded below. A gradient flow model which satisfies energy decay in the direction of steepest descent of energy is a method to solve the minimization problem (2.2). The general form of the gradient flow is given by

$$\begin{cases} \frac{\partial \phi_i(r,t)}{\partial t} = -\frac{\delta E(\Phi)}{\delta \phi_i(r,t)} = f_i \Delta \phi_i(r,t) - V_{KS}(r,t) \frac{\delta \rho}{\delta \phi_i(r,t)}, & r \in \Omega, \quad t > 0, \\ \int_{\Omega} \phi_i(r,t) \phi_j(r,t) dr = \delta_{ij}, & t \geq 0, \end{cases} \quad (2.3)$$

where

$$V_{KS}(r,t) = V_{ext}(r) + V_{Har}(r,t) + V_{xc}(r,t)$$

and  $1 \leq i, j \leq N$ . The above model can also be derived by using imaginary time in the time-dependent Kohn-Sham equation, the detailed derivation is similar to [3]. It is noted that due to orthonormality constraint, iterations based on the above model should be carefully handled. In the next section, we will propose a numerical scheme based on the SAV method to deal with orthonormality constraint. For simplicity, we use  $\phi$  to represent the  $\phi(r,t)$  in the following analysis.

### 3 A numerical scheme based on SAV method and evaluation of potentials

In this section, to handle the orthonormality constraint, we present a modified Kohn-Sham energy functional with two kinds of penalty terms. Then we reformulate the corresponding imaginary time gradient flow into an equivalent form by introducing three kinds of auxiliary variables. For the equivalent form, a designed scheme is adopted for temporal discretization and the finite element method is used for spatial discretization, respectively. Due to the singularity from the external potential, the  $h$ -adaptive mesh method is adopted to save computation resources. The evaluation of Hartree and exchange-correlation potentials is also presented.

#### 3.1 A numerical scheme based on SAV method

It is noted that in [35], the norm constraint was removed by introducing some penalty terms in the total energy. In our work, we try to check this idea still works for orthogonality constraint. Define a linear operator

$$\mathcal{L}: \mathcal{L}\phi_i = -f_i \Delta \phi_i + V_{ext}(r) \delta \rho / \delta \phi_i \quad \text{for } 1 \leq i \leq N,$$

and denote the nonlinear energy functional as

$$\int_{\Omega} F(\rho) dr = E_{xc}(\rho) + E_{har}(\rho).$$

We write a modified Kohn-Sham total energy functional with two kinds of penalty terms as follows

$$\widehat{E}(\Phi) = \frac{1}{2} \sum_{i=1}^N (\phi_i, \mathcal{L}\phi_i) + \int_{\Omega} F(\rho) dr + \frac{1}{4\epsilon} \sum_{i=1}^N \left( \int_{\Omega} |\phi_i|^2 dr - 1 \right)^2 + \frac{1}{2\epsilon} \sum_{i=1}^N \sum_{j=i+1}^N \left( \int_{\Omega} \phi_i \phi_j dr \right)^2, \quad (3.1)$$

where  $\epsilon \ll 1$  and the corresponding gradient flow takes the form

$$\frac{\partial \phi_i}{\partial t} = - \frac{\delta \widehat{E}(\Phi)}{\delta \phi_i} = - \mathcal{L}\phi_i - F'(\rho) \frac{\delta \rho}{\delta \phi_i} - \frac{1}{\epsilon} \left( \int_{\Omega} |\phi_i|^2 dr - 1 \right) \phi_i - \frac{1}{\epsilon} \sum_{\substack{j=1 \\ j \neq i}}^N \left( \int_{\Omega} \phi_i \phi_j dr \right) \phi_j, \quad (3.2)$$

where  $1 \leq i \leq N$ . Assume  $\int_{\Omega} F(\rho) dr$  is bounded from below. To reformulate (3.2), we introduce the following three kinds of scalar auxiliary variables:

$$\begin{cases} u = \sqrt{\int_{\Omega} F(\rho) dr + C_0} \quad (C_0 \geq 0), \\ v_{ii} = \int_{\Omega} |\phi_i|^2 dr - 1, \quad v_{ij} = \int_{\Omega} \phi_i \phi_j dr, \end{cases} \quad (3.3)$$

here  $1 \leq i < j \leq N$ . Then (3.2) can be rewritten as

$$\begin{cases} \frac{\partial \phi_i}{\partial t} = - \left( \mathcal{L}\phi_i + 2u \frac{\delta u}{\delta \phi_i} + \frac{1}{2\epsilon} v_{ii} \frac{\delta v_{ii}}{\delta \phi_i} + \frac{1}{\epsilon} \sum_{\substack{j=1 \\ j \neq i}}^N v_{ij} \frac{\delta v_{ij}}{\delta \phi_i} \right), & 1 \leq i \leq N, \\ \frac{\partial u}{\partial t} = \sum_{i=1}^N \int_{\Omega} \frac{\delta u}{\delta \phi_i} \frac{\partial \phi_i}{\partial t} dr, & 1 \leq i \leq N, \\ \frac{\partial v_{ii}}{\partial t} = \int_{\Omega} \frac{\delta v_{ii}}{\delta \phi_i} \frac{\partial \phi_i}{\partial t} dr, & 1 \leq i \leq N, \\ \frac{\partial v_{ij}}{\partial t} = \int_{\Omega} \left( \frac{\delta v_{ij}}{\delta \phi_i} \frac{\partial \phi_i}{\partial t} + \frac{\delta v_{ij}}{\delta \phi_j} \frac{\partial \phi_j}{\partial t} \right) dr, & 1 \leq i < j \leq N, \end{cases} \quad (3.4)$$

here

$$\begin{cases} \frac{\delta u}{\delta \phi_i} = \frac{1}{2\sqrt{\int_{\Omega} F(\rho) dr + C_0}} \frac{\delta \int_{\Omega} F(\rho) dr}{\delta \rho} \frac{\delta \rho}{\delta \phi_i}, & 1 \leq i \leq N, \\ \frac{\delta v_{ii}}{\delta \phi_i} = 2\phi_i, \quad \frac{\delta v_{ij}}{\delta \phi_i} = \phi_j, \quad \frac{\delta v_{ij}}{\delta \phi_j} = \phi_i, & 1 \leq i < j \leq N. \end{cases} \quad (3.5)$$

Compared with the scheme (2.3), it is noticed that our scheme (3.4) does not have any orthonormality constraint at each time step. Therefore, it is easy to implement.

For temporal discretization, we design the following scheme:

$$\left\{ \begin{aligned} \frac{\phi_i^{n+1} - \phi_i^n}{\Delta t} &= -\frac{\mathcal{L}\phi_i^{n+1} + \mathcal{L}\phi_i^n}{2} - (u^{n+1} + u^n) \frac{\delta u}{\delta \phi_i}(\phi_i^n) - \frac{1}{4\epsilon} (v_{ii}^{n+1} + v_{ii}^n) \frac{\delta v_{ii}}{\delta \phi_i}(\phi_i^n) \\ &\quad - \frac{1}{2\epsilon} \sum_{\substack{j=1 \\ j \neq i}}^N (v_{ij}^{n+1} + v_{ij}^n) \frac{\delta v_{ij}}{\delta \phi_i}(\phi_i^n), & 1 \leq i \leq N, \\ \frac{u^{n+1} - u^n}{\Delta t} &= \sum_{i=1}^N \int_{\Omega} \frac{\delta u}{\delta \phi_i}(\phi_i^n) \frac{\phi_i^{n+1} - \phi_i^n}{\Delta t} dr, & 1 \leq i \leq N, \\ \frac{v_{ii}^{n+1} - v_{ii}^n}{\Delta t} &= \int_{\Omega} \frac{\delta v_{ii}}{\delta \phi_i}(\phi_i^n) \frac{\phi_i^{n+1} - \phi_i^n}{\Delta t} dr, & 1 \leq i \leq N, \\ \frac{v_{ij}^{n+1} - v_{ij}^n}{\Delta t} &= \int_{\Omega} \left( \frac{\delta v_{ij}}{\delta \phi_i}(\phi_i^n) \frac{\phi_i^{n+1} - \phi_i^n}{\Delta t} + \frac{\delta v_{ij}}{\delta \phi_j}(\phi_j^n) \frac{\phi_j^{n+1} - \phi_j^n}{\Delta t} \right) dr, & 1 \leq i < j \leq N. \end{aligned} \right. \quad (3.6)$$

**Remark 3.1.** To preserve the orthonormality, we need sufficiently small  $\epsilon$ . The conclusion is confirmed in our numerical experiments.

Next we show that with the designed scheme given above, the energy decay property can be preserved well, demonstrated by the following theorem.

**Theorem 3.1.** *The scheme (3.6) is unconditionally energy stable in the sense that*

$$\tilde{E}(\Phi^{n+1}, u^{n+1}, v_{ii}^{n+1}, v_{ij}^{n+1}) - \tilde{E}(\Phi^n, u^n, v_{ii}^n, v_{ij}^n) = -\frac{1}{\Delta t} \sum_{i=1}^N \|\phi_i^{n+1} - \phi_i^n\|^2, \quad (3.7)$$

where  $\tilde{E}(\Phi, u, v_{ii}, v_{ij})$  is the modified energy, which is defined as

$$\tilde{E}(\Phi, u, v_{ii}, v_{ij}) = \frac{1}{2} \sum_{i=1}^N (\mathcal{L}\phi_i, \phi_i) + u^2 + \frac{1}{4\epsilon} \sum_{i=1}^N v_{ii}^2 + \frac{1}{2\epsilon} \sum_{i=1}^N \sum_{j=i+1}^N v_{ij}^2. \quad (3.8)$$

*Proof.* Firstly, taking the inner product of the first equation of (3.6) with  $-(\phi_i^{n+1} - \phi_i^n)$ , and summing over  $i$ , and then multiplying the second equation, the third equation and the fourth equation with  $u^{n+1} + u^n$ ,  $v_{ii}^{n+1} + v_{ii}^n$  and  $v_{ij}^{n+1} + v_{ij}^n$ , for  $1 \leq i < j \leq N$ , respectively, finally we obtain the following:

$$\begin{aligned} -\frac{1}{\Delta t} \sum_{i=1}^N \|\phi_i^{n+1} - \phi_i^n\|^2 &= \frac{1}{2} \sum_{i=1}^N (\mathcal{L}\phi_i^{n+1} + \mathcal{L}\phi_i^n, \phi_i^{n+1} - \phi_i^n) + ((u^{n+1})^2 - (u^n)^2) \\ &\quad + \frac{1}{4\epsilon} \sum_{i=1}^N ((v_{ii}^{n+1})^2 - (v_{ii}^n)^2) + \frac{1}{2\epsilon} \sum_{i=1}^N \sum_{j=i+1}^N ((v_{ij}^{n+1})^2 - (v_{ij}^n)^2). \end{aligned} \quad (3.9)$$

Expanding the left hand side of (3.7) by (3.8), then the conclusion can be obtained immediately.  $\square$

**Remark 3.2.** In the previous literatures [32,33,35], it is required that the linear operator  $\mathcal{L}$  is positive definite to preserve the energy decay property, but in our work, the restriction can be removed.

As we discussed in the introduction, the scheme (3.6) can be efficiently solved. Denote

$$\bar{\phi} = (\phi_1, \phi_2, \dots, \phi_N)^T, \quad \bar{v} = (v_{11}, v_{22}, \dots, v_{NN})^T$$

and

$$\bar{w} = (v_{12}, \dots, v_{1N}, v_{23}, v_{24}, \dots, v_{2N}, \dots, v_{N-1,N})^T,$$

respectively. The matrix form of (3.6) can be rewritten as

$$\begin{pmatrix} \left(I + \frac{\Delta t}{2} \mathcal{L}\right)_{\bar{\phi}} & * & * & * \\ * & 1 & 0 & 0 \\ * & 0 & I_{\bar{v}} & 0 \\ * & 0 & 0 & I_{\bar{w}} \end{pmatrix} \begin{pmatrix} \bar{\phi}^{n+1} \\ u^{n+1} \\ \bar{v}^{n+1} \\ \bar{w}^{n+1} \end{pmatrix} = \bar{b}^n, \quad (3.10)$$

where  $I_x$  is the identity operator that depends on the size of the variable  $x$ .  $*$  are the terms with non-constant coefficients.  $\bar{b}^n$  represents the terms from the previous time steps. With the help of block Gaussian elimination method,  $(u^{n+1}, \bar{v}^{n+1}, \bar{w}^{n+1})^T$  can be solved first, which requires solving several times systems of the following form

$$\left(I + \frac{\Delta t}{2} \mathcal{L}\right) \psi = h(x). \quad (3.11)$$

With  $(u^{n+1}, \bar{v}^{n+1}, \bar{w}^{n+1})^T$  known, then we can obtain  $\bar{\phi}^{n+1}$  by solving several systems in the above form. Below is a remark.

**Remark 3.3.** Due to the penalized energy, we do not need to deal with the orthonormality condition at each time step.

To give a fully discretized scheme, we consider the finite element method for spatial discretization. Assume the computational domain  $\Omega$  is bounded and  $(\cdot, \cdot)$  be the inner product in  $L^2(\Omega)$ . For the domain  $\Omega$ , we have a tetrahedron mesh  $\mathcal{T}$  which completely covers the domain  $\Omega$ . The mesh  $\mathcal{T}$  consists of a set of nonoverlapped tetrahedron elements, i.e.,  $\mathcal{T} = \{T_k\}_{k=1}^{N_{tet}}$ , where  $N_{tet}$  is the total number of the tetrahedron elements in the mesh  $\mathcal{T}$ . We define the finite element  $(T_k, \mathcal{P}_1, \mathcal{N})$ , where  $\mathcal{P}_1$  is the set of all first order polynomials in three variables, and  $\mathcal{N}$  is the set of nodal variables. With above notations, we define

$$V_h = \{v \in \mathcal{C}(\Omega) : v \text{ is linear in } T_k \text{ for each } T_k \in \mathcal{T}, v = 0 \text{ on } \partial\Omega\}.$$

Let  $\{W_1, W_2, \dots, W_{N_{basis}}\}$  be the basis functions of the linear Lagrange element space  $V_h \subset H_0^1(\Omega)$  associated with the mesh  $\mathcal{T}$  and

$$\phi_i = \sum_{k=1}^{N_{basis}} \varphi_{i,k} W_k, \quad i = 1, \dots, N. \tag{3.12}$$

Let superscript  $n$  denote the representation of the corresponding term at time  $t = n\Delta t$ .

We obtain the following full discretization of problem (3.4): Given  $\varphi_{i,k}^n$ , find  $\varphi_{i,k}^{n+1} \in V_h$  such that

$$\begin{aligned} & \left[ \sum_{k=1}^{N_{basis}} (W_k, W_m) + \frac{\Delta t}{2} f_i \left( \sum_{k=1}^{N_{basis}} (\nabla W_k, \nabla W_m) + \sum_{k=1}^{N_{basis}} (V_{ext}(r) W_k, W_m) \right) \right] \varphi_{i,k}^{n+1} \\ & + \Delta t u^{n+1} \left( \frac{\delta u}{\delta \phi_i}(\phi_i^n), W_m \right) + \frac{\Delta t}{4\epsilon} v_{ii}^{n+1} \left( \frac{\delta v_{ii}}{\delta \phi_i}(\phi_i^n), W_m \right) + \sum_{j \neq i}^N \frac{\Delta t}{2\epsilon} v_{ij}^{n+1} \left( \frac{\delta v_{ij}}{\delta \phi_i}(\phi_i^n), W_m \right) \\ & = \left[ \sum_{k=1}^{N_{basis}} (W_k, W_m) - \frac{\Delta t}{2} f_i \left( \sum_{k=1}^{N_{basis}} (\nabla W_k, \nabla W_m) + \sum_{k=1}^{N_{basis}} (V_{ext}(r) W_k, W_m) \right) \right] \varphi_{i,k}^n \\ & - \Delta t u^n \left( \frac{\delta u}{\delta \phi_i}(\phi_i^n), W_m \right) - \frac{\Delta t}{4\epsilon} v_{ii}^n \left( \frac{\delta v_{ii}}{\delta \phi_i}(\phi_i^n), W_m \right) - \sum_{j \neq i}^N \frac{\Delta t}{2\epsilon} v_{ij}^n \left( \frac{\delta v_{ij}}{\delta \phi_i}(\phi_i^n), W_m \right), \end{aligned} \tag{3.13a}$$

$$u^{n+1} - \sum_{k=1}^{N_{basis}} \left( \frac{\delta u}{\delta \phi_i}(\phi_i^n), W_k \right) \varphi_{i,k}^{n+1} = u^n - \sum_{k=1}^{N_{basis}} \left( \frac{\delta u}{\delta \phi_i}(\phi_i^n), W_k \right) \varphi_{i,k}^n \tag{3.13b}$$

$$v_{ii}^{n+1} - \sum_{k=1}^{N_{basis}} \left( \frac{\delta v_{ii}}{\delta \phi_i}(\phi_i^n), W_k \right) \varphi_{i,k}^{n+1} = v_{ii}^n - \sum_{k=1}^{N_{basis}} \left( \frac{\delta v_{ii}}{\delta \phi_i}(\phi_i^n), W_k \right) \varphi_{i,k}^n \tag{3.13c}$$

$$\begin{aligned} & v_{ij}^{n+1} - \sum_{k=1}^{N_{basis}} \left( \frac{\delta v_{ij}}{\delta \phi_i}(\phi_i^n), W_k \right) \varphi_{i,k}^{n+1} - \sum_{k=1}^{N_{basis}} \left( \frac{\delta v_{ij}}{\delta \phi_j}(\phi_j^n), W_k \right) \varphi_{j,k}^{n+1} \\ & = v_{ij}^n - \sum_{k=1}^{N_{basis}} \left( \frac{\delta v_{ij}}{\delta \phi_i}(\phi_i^n), W_k \right) \varphi_{i,k}^n - \sum_{k=1}^{N_{basis}} \left( \frac{\delta v_{ij}}{\delta \phi_j}(\phi_j^n), W_k \right) \varphi_{j,k}^n \end{aligned} \tag{3.13d}$$

where  $m = 1, 2, \dots, N_{basis}$ .

### 3.2 Evaluation of potentials

In this subsection, we present the evaluation of three potentials, which are used to compute the operator  $\mathcal{L}$  and the scalar auxiliary variable  $u$  in scheme (3.6), respectively. Below we introduce the external potential first.

Notice that there exists singularity from the external potential  $V_{ext}(r)$ , therefore, the adaptive mesh is a good choice for a quality description of it. In our work, we choose the  $h$ -adaptive finite element method. The general process of adaptive algorithm with a *posteriori* error estimate includes:

$$\dots \rightarrow \text{Solution} \rightarrow \text{Error estimation} \rightarrow \text{Mark} \rightarrow \text{Refinement} \rightarrow \dots$$

More specifically, firstly we need to solve (3.13a) on the current mesh  $\mathcal{T}_k$  to obtain an approximate solution and compute an error indicator  $\eta_{T_k}$ . Then by using the error indicator and Dörfler's marking strategy [11], some elements would be marked and these marked elements would be refined later. Finally, a new finite element space  $\mathcal{T}_{k+1}$  will be built and the numerical solution will be updated from the old space to the new space. To handle the singularity well, the following error indicator is designed based on numerical experience

$$\eta_{T_k} = \int_{T_k} |\nabla\Phi|^2 dr + \int_{T_k} \frac{Z_M}{|r-R_M|^3} dr, \quad (3.14)$$

here  $T_k$  is the  $k$ -th element on the mesh  $\mathcal{T}$  and  $Z_M$  is the charge of the  $M$ -th nucleus.  $R_M$  is the position of the  $M$ -th nucleus. Note that the first term in (3.14) represents the integral of the wave function gradient in the current element and the second part exists to describe the singularity from external potential well. By normalizing the two terms of the above indicator respectively, the proportions of them tend to balance.

In our numerical experiments, the Hartree potential is obtained by solving the following Poisson equation,

$$-\nabla^2 V_{Har} = 4\pi\rho, \quad (3.15)$$

and its boundary values are given by multipole expansion approximation [2].

Moreover, the exchange-correlation potential is obtained with the local density approximation (LDA) [28]. Suppose

$$E_{xc}(\rho) = \int_{\Omega} \epsilon_{xc}(\rho)\rho dr,$$

then we have

$$V_{xc} = \epsilon_{xc}(\rho) + \rho \frac{\delta\epsilon_{xc}}{\delta\rho}, \quad (3.16)$$

where  $\epsilon_{xc}(\rho) = \epsilon_x(\rho) + \epsilon_c(\rho)$  with

$$\epsilon_x(\rho) = \frac{3}{4} \left( \frac{3}{\pi} \right)^{\frac{1}{3}} \rho^{\frac{1}{3}} \quad (3.17)$$

and

$$\epsilon_c(\rho) = \begin{cases} -0.1423r_s / (r_s + 1.0529\sqrt{r_s} + 0.3334), & \text{if } r_s < 1, \\ -0.0311\ln r_s - 0.048 + 0.0020\ln r_s / r_s - 0.0116 / r_s, & \text{if } r_s \geq 1, \end{cases} \quad (3.18)$$

here  $r_s = (4\pi\rho/3)^{1/3}$ .

## 4 Numerical experiments

All numerical experiments are implemented by using iFEM [6] on a Dell OptiPlex 7060 with the configuration: Inter(R) Core(TM) i7-8700 CPU @3.20 GHz and 8.00 GB of memory. For the test, we set the computational domain  $\Omega = [-10, 10]^3$ . The stopping criterion

for the ground state solution is  $|E_{n+1} - E_n| < 1.0e-06$ . The initial condition is given by  $\phi_i(r,0) = ae^{-b|r-R_i|}$ ,  $i = 1, 2, \dots, N$ ,  $a = 1$  and  $b = 2$ . The occupation of orbital  $i$  is  $f_i = 2$ . We give the following three examples to validate the effectiveness of our scheme (3.6),

- A helium (He) atom consists of 1 nucleus with charge 2 and location  $(0,0,0)$ , 2 electrons;
- A lithium-hydrogen (LiH) molecule consists of 2 nuclei with charges  $\{1,3\}$  and locations  $(c_1,0,0)$  and  $(c_2,0,0)$ , respectively, and 4 electrons, where  $c_1 = -1.0075$  and  $c_2 = 2.0075$ ;
- A methane (CH<sub>4</sub>) molecule consists of 5 nuclei with charges  $\{6,1,1,1,1\}$  and locations  $(0,0,0)$ ,  $(c_3,c_3,c_3)$ ,  $(-c_3,-c_3,c_3)$ ,  $(c_3,-c_3,-c_3)$ ,  $(-c_3,c_3,-c_3)$ , respectively, and 10 electrons, where  $c_3 = 1.3092$ .

### 4.1 Convergence

In this subsection, both the spatial and temporal convergence behavior of our scheme (3.6) can be observed. We begin by studying the temporal convergence behavior. We set  $\epsilon = 1.0e-05$  and compare the performances on a fixed nonuniform mesh with different time steps  $\Delta t$ . To obtain a reference energy, we use the scheme (3.6) with a small time step  $\Delta t = 2.5e-04$ . The reference energies for three examples we used are  $-2.831859$  hartrees,  $-7.891271$  hartrees,  $-38.655774$  hartrees, respectively. Here a hartree is a unit of energy used in molecular orbital calculations.  $T_{\max}$  is the moment when the reference energy reaches the ground state. The energy error is calculated by  $E_{err} = |E_{reference} - E_{numerical}|$ . Table 1 shows the iteration numbers and energy errors at  $T_{\max} = 0.7760, 2.0940, 1.6173$  for three examples with different time steps  $\Delta t$ , respectively. It can be observed that the iteration number grows with the increment of time step  $\Delta t$ . Moreover, the temporal convergence of energy behavior can also be obtained.

To show spatial convergence behavior, we set  $\epsilon = 1.0e-05$  and fix  $\Delta t = 2.5e-04$ . Fig. 1 shows the performance of the He atom. The convergence curves of the approximated energy behave can be observed as expected from the top subfigure of Fig. 1 and the final result we obtained is  $-2.831859$  hartrees. The bottom left subfigure of Fig. 1 shows the

Table 1: Iteration numbers and energy errors with different time steps  $\Delta t$ .

$\Delta t$	He atom		LiH molecule		CH <sub>4</sub> molecule	
	Iteration	$E_{err}$	Iteration	$E_{err}$	Iteration	$E_{err}$
8.0e-03	98	1.2654	263	0.3512	199	3.8426
4.0e-03	195	6.0991e-01	525	2.2400e-02	396	7.3903e-01
2.0e-03	389	2.7627e-02	1048	4.6956e-04	790	1.4923e-03
1.0e-03	777	3.7727e-05	2095	1.8183e-04	1578	1.0037e-04
2.5e-04	3105	-	8377	-	6307	-

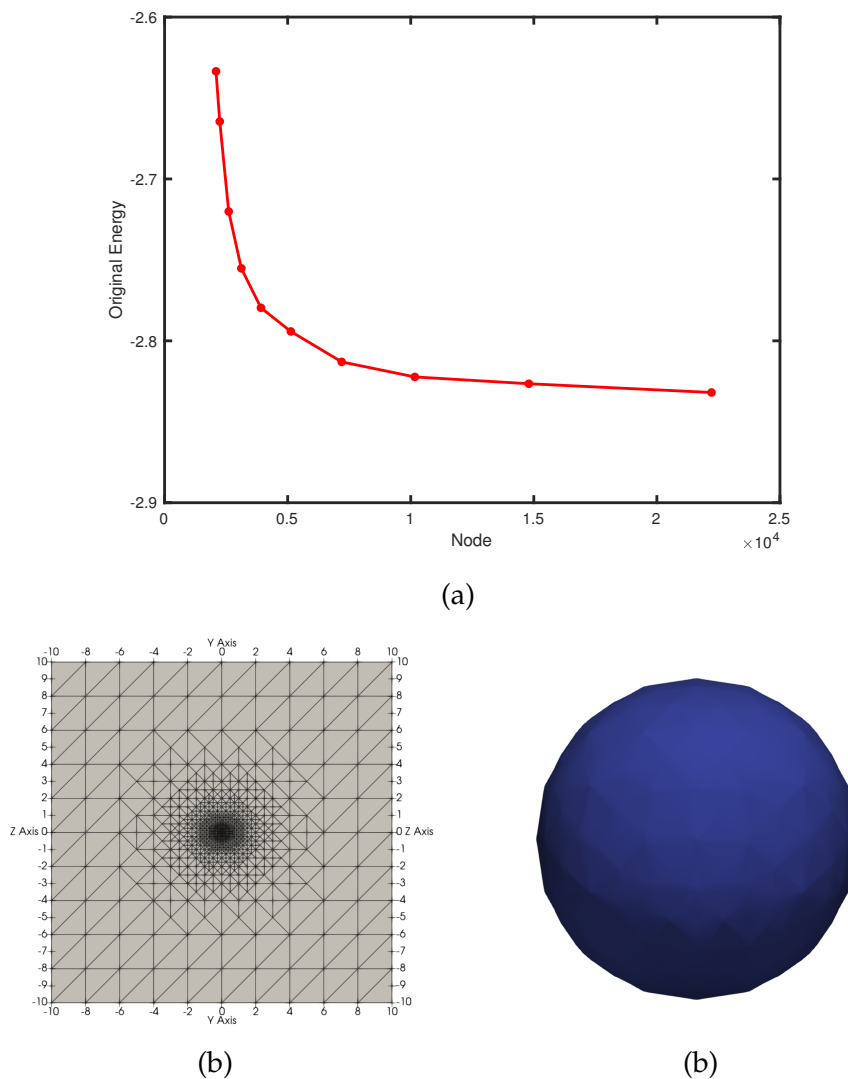


Figure 1: The performance of the He atom. (a): Evolution of original energy for the He atom in an adaptive mesh. (b): The mesh distribution for the He atom in the tangent plane  $x=0$ ; (c): The contour of the electron density of the He atom.

final mesh distribution in the tangent plane  $x=0$ , it can be seen that more grids are centered around the position of the nucleus. The contour of the electron density is shown in the bottom right part of Fig. 1. The performance of the LiH molecule is shown in Fig. 2. Similar to the He atom, from the top subfigure of Fig. 2, it can be obtained that the approximations of original energy are convergent and the final energy we obtained is  $-7.893865$  hartrees. Compared with the value  $-7.933035$  hartrees in the database [18], there is only 0.4% difference. The bottom left subfigure of Fig. 2 shows the densest mesh

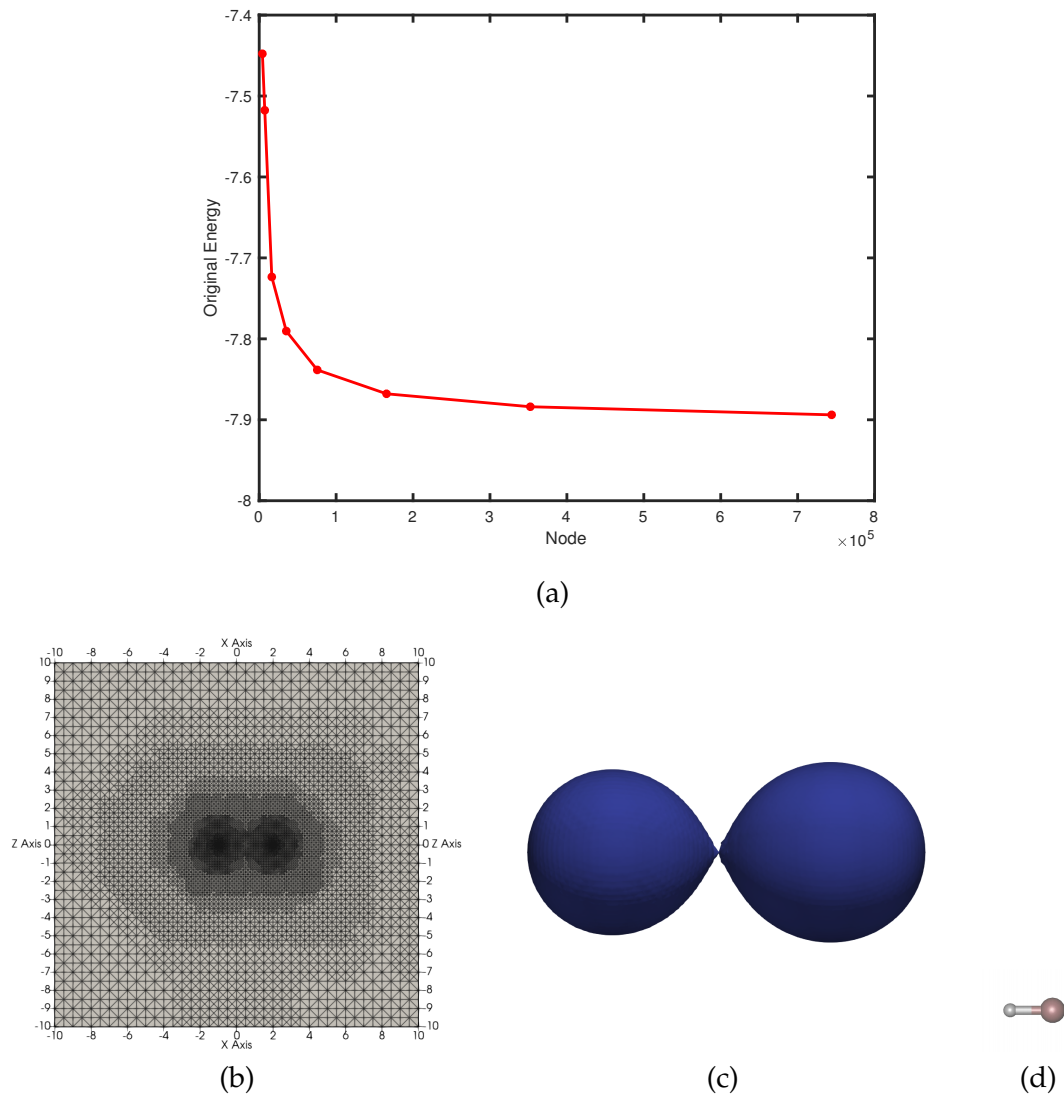


Figure 2: The performance of the LiH molecule. (a): Evolution of original energy for the LiH molecule in an adaptive mesh. (b): The mesh distribution for the LiH molecule in the tangent plane  $y=0$ ; (c): The contour of the electron density of the LiH molecule; (d): Reference molecular structure of LiH molecule [10].

distribution in the tangent plane ( $y=0$ ). It can be seen that the two singularities are well captured. The contour of the electron density and the reference molecular structure [10] are shown in the bottom middle and right subfigures of Fig. 2, respectively. Fig. 3 shows the performance of the  $\text{CH}_4$  molecule. The same spatial convergence of energy behavior can be obtained from the top part of Fig. 3 as previous examples. The final energy of the  $\text{CH}_4$  molecule we obtained is  $-39.962142$  hartrees, which is close to the experimental

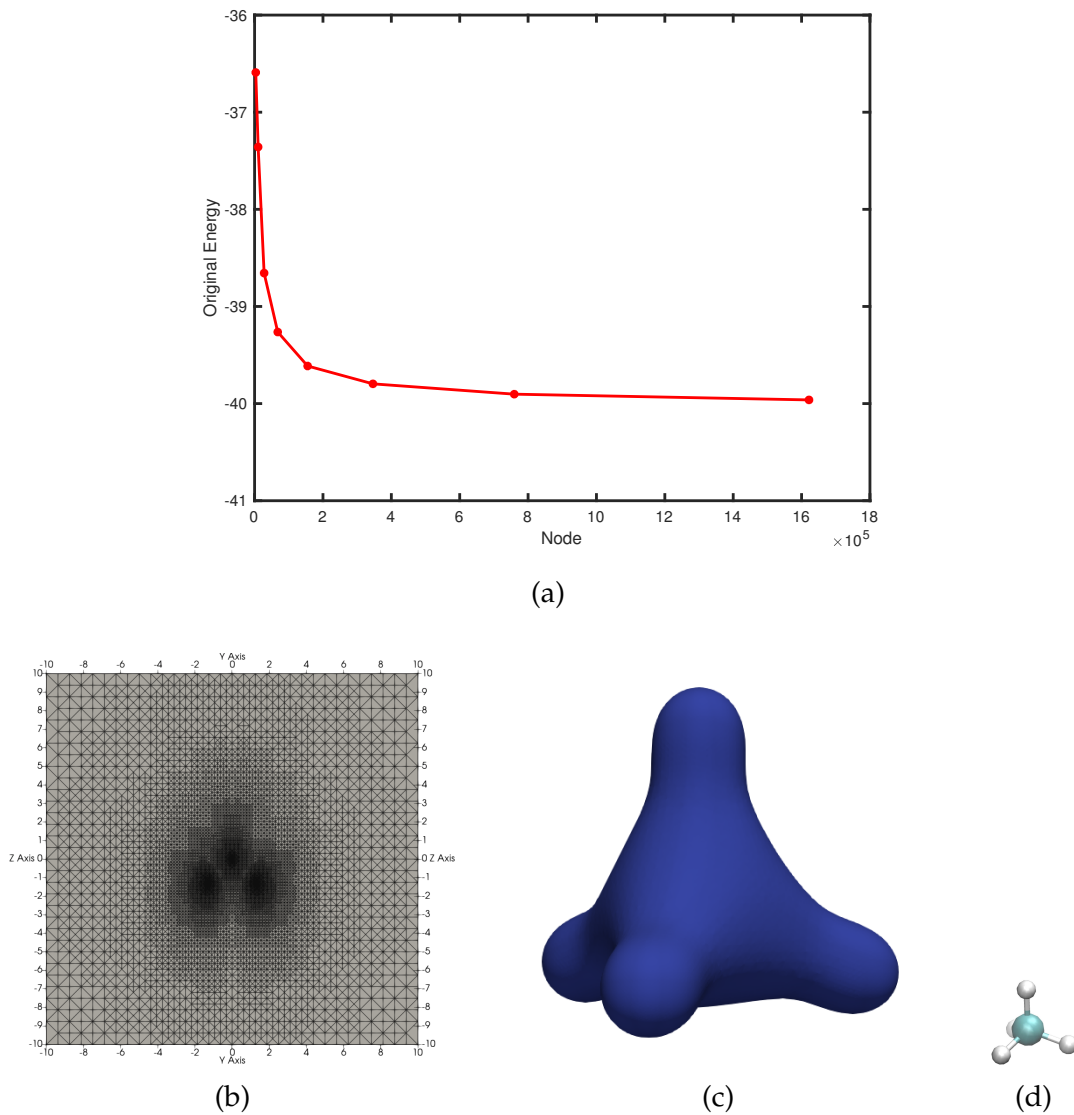


Figure 3: The performance of the CH<sub>4</sub> molecule. (a): Evolution of original energy for the CH<sub>4</sub> molecule in an adaptive mesh. (b): The mesh distribution for the CH<sub>4</sub> molecule in the tangent plane  $x+y=0$ ; (c): The contour of the electron density of the CH<sub>4</sub> molecule; (d): Reference molecular structure of CH<sub>4</sub> molecule [10].

values from the database [18]. And the corresponding mesh distribution in the tangent plane  $x+y=0$  is shown in the bottom left part of Fig. 3, where the original is the position of the carbon atom, and other two singularities are the positions of the hydrogen atoms. The contour of the electron density and the reference molecular structure [10] are shown in the bottom middle and right subfigures of Fig. 3, respectively.

### 4.2 Energy stability

In the previous section, the energy decay property of our scheme (3.6) has been proved by Theorem 1. In this subsection, the property can also be observed from our experiments. We set  $\epsilon = 1.0e-5$  and  $\Delta t = 2.5e-04$  and still test on a fixed nonuniform mesh. The evolution of the original energy  $E$  and modified energy  $\tilde{E}$  by scheme (3.6) for three examples are shown in Fig. 4. Although we can only prove the modified energy decay theoretically, both original total energy and modified total energy decay behaviors can be observed numerically.

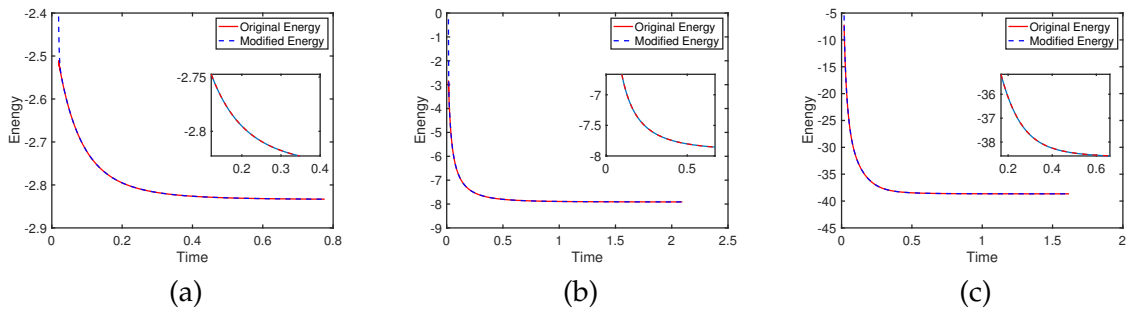


Figure 4: Evolution of original and modified energies for three examples.  $\epsilon = 1.0e-05$ ,  $\Delta t = 2.5e-04$ . (a): the He atom; (b): the LiH molecule; (c): the CH<sub>4</sub> molecule.

### 4.3 Orthonormality

In this subsection, orthonormality relationships among wave functions can be shown numerically. That is, our solutions obtained from the scheme (3.6) can keep the orthonormality naturally by introducing two kinds of penalty terms into the Kohn-Sham energy functional. It is worth mentioning that such a strategy avoids dealing with orthonormality constraint at each time step, which shows the potential for saving computation resources. The norm and orthogonality persevering are illustrated by the indications defined as  $\max_{1 \leq i \leq N} |||\phi_i||^2 - 1|$  and  $\max_{1 \leq i < j \leq N} |(\phi_i, \phi_j)|$ , respectively. We set  $\Delta t = 2.5e-04$  and let  $\epsilon$  vary from  $1.0e-04$  to  $1.0e-06$  and still test on a fixed nonuniform mesh.

Table 2 shows the value of  $\max_{1 \leq i \leq N} |||\phi_i||^2 - 1|$  with different  $\epsilon$  for three examples. It can be seen that the norm constraint of each wave function is preserved well. Moreover, it can be obtained that the value of  $\max_{1 \leq i < j \leq N} |||\phi_i||^2 - 1|$  depends linearly on  $\epsilon$ , which is consistent with Remark 3.1. The orthogonality of wave functions for two molecules are shown in Table 3. It is clearly seen from the table that besides the norm-preserving of each wave function, the orthogonality between each pair of different wave functions is preserved well. Similarly, the value of  $\max_{1 \leq i < j \leq N} |(\phi_i, \phi_j)|$  also depends linearly on  $\epsilon$ . A similar conclusion can be obtained from Table 3 as the previous table.

Table 2: The values  $\max_{1 \leq i \leq N} \|\phi_i\|^2 - 1$  with different  $\epsilon$  for the He atom, the LiH molecule and the CH<sub>4</sub> molecule, respectively.

$\epsilon$	He atom	LiH molecule	CH <sub>4</sub> molecule
1.0e-04	2.3871e-04	7.4365e-04	3.8000e-03
1.0e-05	2.3882e-05	7.4427e-05	3.7794e-04
1.0e-06	2.3827e-06	7.4424e-06	3.7801e-05

Table 3: The values  $\max_{1 \leq i < j \leq N} |(\phi_i, \phi_j)|$  with different  $\epsilon$  for the LiH molecule and the CH<sub>4</sub> molecule, respectively.

$\epsilon$	LiH molecule	CH <sub>4</sub> molecule
1.0e-04	6.4970e-05	3.1544e-05
1.0e-05	6.5080e-06	3.1555e-06
1.0e-06	6.4590e-07	3.1556e-07

## 5 Conclusions

In this paper, based on the imaginary time gradient flow model, we proposed an unconditionally energy stable scheme for the ground state calculation of a given electronic structure system by using the SAV method. To avoid dealing with the orthonormality constraint of wave functions at each time step, we designed a modified Kohn-Sham energy functional by introducing two kinds of penalty terms and our numerical results successfully showed the effectiveness of this strategy. Although we can only prove the modified energy decay theoretically, both the original total energy and modified energy decay behaviors can be observed numerically.

It can be obtained from the numerical results that we should take much smaller  $\epsilon$  to preserve the orthonormality relationships between wave functions, which raises the requirement of sufficiently small  $\Delta t$  during time propagation. For future work, we will study some acceleration strategies to improve the simulation.

## Acknowledgements

The first author would like to thank the support from the UM-Funded PhD Assistantship from University of Macau. The second author was partially supported by Macao Young Scholar Program (AM201919), excellent youth project of Hunan Education Department (19B543) and Hunan National Applied Mathematics Center of Hunan Provincial Science and Technology Department (2020ZYT003). The third author would like to thank financial support from National Natural Science Foundation of China (Grant Nos. 11922120, 11871489), FDCT of Macao SAR (Grant No. 0082/2020/A2), University of Macau (Grant No. MYRG2020-00265-FST), and Guangdong-Hong Kong-Macao Joint Laboratory for Data-Driven Fluid Mechanics and Engineering Applications (Grant

No. 2020B1212030001).

## References

- [1] X. ANTOINE, J. SHEN, AND Q. TANG, *Scalar auxiliary variable/ Lagrange multiplier based pseudospectral schemes for the dynamics of nonlinear Schrödinger/ Gross-Pitaevskii equations*, J. Comput. Phys., 437 (2021), p. 110328.
- [2] G. BAO, G. HU, AND D. LIU, *Numerical solution of the Kohn-Sham equation by finite element methods with an adaptive mesh redistribution technique*, J. Sci. Comput., 55 (2013), pp. 372–391.
- [3] W. BAO AND Q. DU, *Computing the ground state solution of Bose–Einstein condensates by a normalized gradient flow*, SIAM J. Sci. Comput., 25 (2004), pp. 1674–1697.
- [4] H. BIAN, Y. SHEN, AND G. HU, *An  $h$ -adaptive finite element solution of the relaxation non-equilibrium model for gravity-driven fingers*, Adv. Appl. Math. Mech., 13 (2021), pp. 1418–1440.
- [5] H. CHEN, X. DAI, X. GONG, L. HE, AND A. ZHOU, *Adaptive finite element approximations for Kohn–Sham models*, Multiscale Model. Simul., 12 (2014), pp. 1828–1869.
- [6] L. CHEN, *iFEM: an integrated finite element methods package in MATLAB*, Technical Report, University of California at Irvine, (2009).
- [7] Q. CHENG, C. LIU, AND J. SHEN, *Generalized SAV approaches for gradient systems*, J. Comput. Appl. Math., 394 (2021), p. 113532.
- [8] Q. CHENG AND C. WANG, *Error estimate of a second order accurate scalar auxiliary variable (SAV) numerical method for the epitaxial thin film equation*, Adv. Appl. Math. Mech., 13 (2021), pp. 1318–1354.
- [9] X. DAI, Z. LIU, X. ZHANG, AND A. ZHOU, *A parallel orbital-updating based optimization method for electronic structure calculations*, J. Comput. Phys., 445 (2021), p. 110622.
- [10] X. DAI, Q. WANG, AND A. ZHOU, *Gradient flow based discretized Kohn-Sham density functional theory*, Multiscale Model. Simul., 18 (2020), pp. 1621–1663.
- [11] W. DÖRFLER, *A convergent adaptive algorithm for Poisson’s equation*, SIAM J. Numer. Anal., 33 (1996), pp. 1106–1124.
- [12] X. FENG, B. LI, AND S. MA, *High-order mass- and energy-conserving SAV-Gauss collocation finite element methods for the nonlinear Schrödinger equation*, SIAM J. Numer. Anal., 59 (2021), pp. 1566–1591.
- [13] C. FIOLEIS, F. NOGUEIRA, AND M. A. MARQUES, *A Primer in Density Functional Theory*, Springer Science & Business Media, 2003.
- [14] B. GAO, G. HU, Y. KUANG, AND X. LIU, *An orthogonalization-free parallelizable framework for all-electron calculations in density functional theory*, SIAM J. Sci. Comput., 44 (2022), pp. B723–B745.
- [15] B. GAO, X. LIU, AND Y. YUAN, *Parallelizable algorithms for optimization problems with orthogonality constraints*, SIAM J. Sci. Comput., 41 (2019), pp. A1949–A1983.
- [16] Y. GONG, J. ZHAO, AND Q. WANG, *Arbitrarily high-order unconditionally energy stable schemes for gradient flow models using the scalar auxiliary variable approach*, Comput. Phys. Commun., 249 (2020), p. 107033.
- [17] F. HUANG, J. SHEN, AND Z. YANG, *A highly efficient and accurate new scalar auxiliary variable approach for gradient flows*, SIAM J. Sci. Comput., 42 (2020), pp. A2514–A2536.
- [18] R. D. JOHNSON III, *NIST Computational Chemistry Comparison and Benchmark Database*, NIST Standard Reference Database Number 101 Release 22, May 2022, <https://cccbdb.nist.gov/energy2x.asp>.

- [19] R. JORDAN, D. KINDERLEHRER, AND F. OTTO, *The variational formulation of the Fokker–Planck equation*, SIAM J. Math. Anal., 29 (1998), pp. 1–17.
- [20] L. JU, X. LI, AND Z. QIAO, *Generalized SAV-exponential integrator schemes for Allen-Cahn type gradient flows*, SIAM J. Numer. Anal., 60 (2022), pp. 1905–1931.
- [21] L. JU, X. LI, AND Z. QIAO, *Stabilized exponential-SAV schemes preserving energy dissipation law and maximum bound principle for the Allen-Cahn type equations*, J. Sci. Comput., 92 (2022), p. 66.
- [22] W. KOHN AND L. J. SHAM, *Self-consistent equations including exchange and correlation effects*, Phys. Rev., 140 (1965), p. A1133.
- [23] Y. KUANG AND G. HU, *On stabilizing and accelerating SCF using ITP in solving Kohn–Sham equation*, Commun. Comput. Phys., 28 (2020), pp. 999–1018.
- [24] Y. KUANG, Y. SHEN, AND G. HU, *An h-adaptive finite element method for Kohn-Sham and time-dependent Kohn-Sham equations*, J. Numer. Methods Comput. Appl., 42 (2021), pp. 33–55.
- [25] Q. LI AND L. MEI, *Efficient, decoupled, and second-order unconditionally energy stable numerical schemes for the coupled Cahn–Hilliard system in copolymer/homopolymer mixtures*, Comput. Phys. Commun., 260 (2021), p. 107290.
- [26] X. LIU, Z. WEN, X. WANG, M. ULBRICH, AND Y. YUAN, *On the analysis of the discretized Kohn–Sham density functional theory*, SIAM J. Numer. Anal., 53 (2015), pp. 1758–1785.
- [27] F. OTTO, *The geometry of dissipative evolution equations: the Porous Medium equation*, Commun. Partial Differential Equations, 26 (2001), pp. 101–174.
- [28] J. P. PERDEW AND A. ZUNGER, *Self-interaction correction to density-functional approximations for many-electron systems*, Phys. Rev. B, 23 (1981), p. 5048.
- [29] Z. QIAO, S. SUN, T. ZHANG, AND Y. ZHANG, *A new multi-component diffuse interface model with Peng-Robinson equation of state and its scalar auxiliary variable (SAV) approach*, Commun. Comput. Phys., 26 (2019), pp. 1597–1616.
- [30] F. SANTAMBROGIO, *Optimal Transport for Applied Mathematicians*, Birkäuser, NY, 55 (2015), p. 94.
- [31] J. SHEN AND J. XU, *Convergence and error analysis for the scalar auxiliary variable (SAV) schemes to gradient flows*, SIAM J. Numer. Anal., 56 (2018), pp. 2895–2912.
- [32] J. SHEN, J. XU, AND J. YANG, *The scalar auxiliary variable (SAV) approach for gradient flows*, J. Comput. Phys., 353 (2018), pp. 407–416.
- [33] J. SHEN, J. XU, AND J. YANG, *A new class of efficient and robust energy stable schemes for gradient flows*, SIAM Rev., 61 (2019), pp. 474–506.
- [34] L. YANG, Y. SHEN, Z. HU, AND G. HU, *An implicit solver for the time-dependent Kohn-Sham equation*, Numer. Math. Theor. Meth. Appl., 14 (2021), pp. 261–284.
- [35] Q. ZHUANG AND J. SHEN, *Efficient SAV approach for imaginary time gradient flows with applications to one-and multi-component Bose-Einstein Condensates*, J. Comput. Phys., 396 (2019), pp. 72–88.